Twelfth Australasian Fluid Mechanics Conference
The University of Sydney, Australia 1995

THE LATERAL ADVANCE SPEED OF THERMOHALINE INTRUSIONS

Barry R. Ruddick
Department of Oceanography
Dalhousie University
Halifax, Nova Scotia
CANADA

ABSTRACT

Ruddick and Turner (*Deep-Sea Research*, 26A, 903-913, 1979) presented a laboratory model of oceanic thermohaline fronts in which lateral density-compensating differences of sugar (S) and salinity (T) concentrations allowed quasi-horizontal intrusive motions to grow. They gave potential energy arguments based on the redistribution of T and S by double-diffusive vertical fluxes that successfully predicted the vertical scale of the intrusions.

These experiments gave further information on the velocity of the intrusions, and hence on the lateral fluxes of T and S. These results are shown for the above experiments, resulting in a prediction of intrusion speed. This speed is compared to predictions from theoretical models, and from observations of the decay of a Mediterranean Salt lens.

INTRODUCTION

Stommel and Fedorov (1967) discovered the presence of temperature-compensated salinity inversions during early use of the continuously recording CTD, and interpreted these as indicative of lateral mixing processes. Their small vertical scale caused Stommel and Fedorov to suggest that vertical mixing blended the features into their new surroundings after lateral advection. Fedorov's (1978) compilation of oceanic observations showed how frequently intrusions occur, and in several instances showed lateral coherence over several kilometers. One set of observations (fig. 6 of that monograph) indicated that intrusions may migrate across isopycnals as they extend laterally. This was also observed later by Gregg (1980) and by Ruddick (1992).

The underlying mechanisms were illuminated in a laboratory experiment by Turner (1978), in which a plume of sugar solution (S) was released into a salinity-stratified tank ($T(z)$). The plume formed a series of laterally-intruding layers consisting of alternating bands of "sugar" fingers and diffusive interfaces (fig. 1). The feedback mechanism that allows such layers to form involves lateral advection and vertical double-diffusive fluxes in the following way:

1. Lateral advection creates alternately high-S and low-S layers, forming fingering and double-diffusive vertical stratifications between the layers.

2. Vertical mixing (Fig. 2) – The finger fluxes cause the high-S layer to lose S and become less dense, with opposite changes in the low-S layer. The diffusive fluxes cause the high-S layer to also lose S but to become more dense, also with opposite changes in the low-S layer. Thus the combined effect of vertical fluxes is to reduce the $T - S$ contrast, and to cause the high-S layer to become less or more dense according to whether the finger or diffusive buoyancy fluxes are larger.

3. If the finger buoyancy fluxes dominate, the high-S layer rises as it moves laterally across, causing a slope in the sense shown in figures 1 and 2. The reverse slope occurs if the diffusive buoyancy fluxes dominate. This was demonstrated when Turner (1978) released a plume of high-T solution into a sugar stratification.

4. The buoyancy flux divergences create density perturbations that combine with the intrusion slopes to create pressure perturbations that drive the advection.

Intrusion models have been proposed that predict vertical scales (Ruddick and Turner, 1978) or linear growth rates and scales (Toole and Georgi, 1981, McDougall, 1985a, Niino. 1986, Walsh and Ruddick, 1994). These models are linearized, neglect the diffusive fluxes, and therefore predict indefinite exponential growth. Since e-folding times are of the order

of a day, and oceanic fronts can exist for several hundred days or more, it seems likely that intrusions grow until a finite-amplitude balance is achieved that controls the amplitude and therefore the lateral intrusive fluxes. It is important to know how large this finite-amplitude state is, and what controls it in order to assess the magnitude of the cross-frontal fluxes.

We describe in the following section the laboratory model of frontal intrusions originally reported in Ruddick and Turner (1978). That paper focused on the vertical scale of the intrusions, and on a simple energy argument for that scale. Each of the intrusions in that experiment was observed to advance at a steady rate. In this report we investigate the scaling rules for that advance speed and the consequences for the lateral fluxes of T and S.

EXPERIMENTAL SETUP

The laboratory setup allowed the creation of a sharp thermohaline front with a controllable variety of vertical stratifications. The experimental tank, 1.8 m × 0.03 m × 0.2 m, made of 6 mm float glass, is shown in fig. 3. A watertight vertical barrier was mounted in the center in such a way that it could be withdrawn vertically by an electric motor at a rate of 2 mm s^{-1}. A row of holes was provided in the top of the barrier, just below the free surface, to allow the water levels to adjust.

Two identical "double bucket" filling systems were used to provide identical linear density gradients of sugar solution on the left, and salt solution on the right. After the two halves of the tank were filled, the barrier was withdrawn a few millimeters to allow the pressures at the bottom to equalize, before the complete withdrawal at the start of the experiment. After withdrawal and slight adjustments of the density field due to imperfections in the density gradients, the experimental setup consisted of sugar stratification on the left, salt stratification on the right, with identical buoyancy frequency N. The thermohaline front down the middle has a salinity contrast $\beta\Delta S$ that increases linearly with depth.

The evolution of the fronts was recorded photographically using the shadowgraph technique, in which light from a projector passing through the tank is deflected by the gradients of the refractive index in the field. The light which falls on tracing paper affixed to the front of the tank is focused by the gradients to clearly show the double-diffusive structures (fig. 4). The position of each intruding nose was monitored closely, and the fluid velocity was measured at selected times by monitoring the displacement of vertical dye streaks produced by dropping potassium permanganate crystals.

RESULTS

After the barrier was withdrawn, the slight inequalities in the density field adjusted via internal waves, which decayed within a few minutes. The thermohaline front which remained was the site of small-scale (i.e., mm-scale) turbulent motions driven by the difference in T and S diffusivities. These became increasingly organized so that after 5–10 minutes a sequence of interleaving layers formed with the structure shown in fig. 1. After formation, each of the layers was observed to extend outwards from the front at a steady rate (fig. 5). The use of colour polarimetry (Ruddick, 1981) in conjunction with the shadowgraph showed that the T/S front filled the region between the noses as sketched in the middle panel of fig. 1, so that the lateral gradient weakened and stayed approximately linear as the noses extended. Thus, the lateral salt flux at the center of the front is given by $c\beta\Delta S/4$ where c is the lateral advance speed of the noses. The constancy of c with time means that the lateral S (and T) flux is constant in time, and does not decrease as the lateral gradient decreases. In other words, the horizontal diffusivity increases as the front broadens!

Several experiments were performed in which $\beta\Delta S$ was proportional to the depth D below the free surface, which can be related to the cross-frontal S-contrast:

$$D = g\beta\Delta S/N^2, \tag{1}$$

where $N = -g/\rho d(\rho)/dz^{1/2}$ is the buoyancy frequency characterizing the stratification strength. The speed of advance c of each nose was observed to be constant in time, and proportional to D. Dimensional reasoning would suggest that all such experiments should evolve in a similar fashion, the only difference between them being that time should scale as N^{-1}. It follows then, that c should be proportional to ND. This scaling hypothesis is tested in figure 6, in which c/N is plotted against D from several experiments. The data exhibit considerable scatter, but are roughly consistent with the relationship shown by the solid line:

$$c/N = 0.0009D - 0.0027cm. \tag{2}$$

We believe the offset (–0.0027) is related to the increased influence of diffusive interfaces near the top of the tank (small D), where the layers are small, or occasionally do not form at all. For the purpose of extrapolation to the oceanic situation, that factor should probably be ignored.

Ruddick and Turner (1978) showed that H was proportional to D, and presented energy arguments for the constant of proportionality. Their formula for the layer thickness H was

$$H = 3/2(1-n)D \tag{3}$$

Where $n = 0.88$ is the flux ratio for sugar-salt fingers. In terms of the layer thickness, the formula for the nose velocity becomes

$$c = 0.005NH. \tag{4}$$

In expressing the laboratory results as in eq. 4, we are implicitly assuming that changing the flux ratio n from 0.88 (the sugar-salt value) to the oceanic value (roughly 0.56) may affect H, but not affect the relationship (4).

DISCUSSION

Since NH is the speed of internal gravity waves of vertical scale H, c/NH is effectively the Froude number of the intrusions. The laboratory observation that intrusions advance with a constant Froude number suggests on the one hand that their dominant physics may involve a a balance between inertia and buoyancy forces. On the other hand, the Froude number is much smaller than is observed for gravity currents, and this may be taken to suggest that the balance is between buoyancy and frictional forces. Models supposing both balances have been devised (Phillips, pers. comm., McDougall, 1985b, Walsh and Ruddick, ms. in prep.) which in either case predict a constant Froude number, and it appears to be difficult to discriminate between them.

Armi *et al.* (1989) describe the evolution over a two-year period of a lens of anomalously warm, saline Mediterranean water that was tracked in the Eastern North Atlantic. They concluded that the primary mode of mixing of the lens into the surrounding waters was via intrusions, and Ruddick (1992) concluded that their driving force was the buoyancy release via double-diffusion. Ruddick and Hebert (1988) estimated the erosion speed to be 1 mm/s, and found that this compared favorably to the speed of advance of thermohaline intrusions given by eq. 4 above.

CONCLUSION

The laboratory experiments described in Ruddick and Turner (1978) were further analyzed with respect to the lateral advance speed of the intrusive motions. This speed was found to be constant in time and proportional to NH, where N is the buoyancy frequency and H is the intrusion thickness. This scaling is predicted by models which suppose that the buoyancy effects are balanced either by inertia or by friction, and compares favorably with the observed decay of a Mediterranean salt lens.

REFERENCES

Armi, L., D. Hebert, N. Oakey, J. Price, P. Richardson, T. Rossby, and B. Ruddick, 1989. Two years in the life of a Mediterranean salt lens. *J. Phys. Oceanogr.*, 19, 354- 370.

Fedorov, K. N. 1978. *The thermohaline finestructure of the ocean.* English Translation, Pergamon Press, Oxford, 169 pp.

Gregg, M.C. 1980. Three-dimensional mapping of a small thermohaline intrusion. *J. Phys. Oceanogr.*, 10, 1468-1492.

McDougall, T.J., 1985a. Double-diffusive interleaving. Part I: Linear stability analysis. *J. Phys. Oceanogr.*, 15, 1532-1541.

McDougall, T.J., 1985b. Double-diffusive interleaving. Part II: Finite-amplitude, steady- state interleaving. *J. Phys. Oceanogr.*, 15, 1542-1556.

Niino, H., 1986. A linear stability theory of double-diffusive horizontal intrusions in a temperature-salinity front. *J. Fluid Mech.*, 171, 71-100.

Ruddick, B.R. (1981) The "colour polarigraph" - a simple method for determining the two dimensional distribution of sugar concentration. J. Fluid Mech., 109, 277-282.

Ruddick B.R. 1992. Intrusive mixing in a Mediterranean salt lens – Intrusion slopes and dynamical mechanisms. *J. Phys. Oceanogr.*, 22, 1274-1285.

Ruddick, B.R., and D. Hebert, 1988. The mixing of Meddy "Sharon". Small-scale mixing in the ocean, J.C.J. Nihoul and B.M. Jamart, Eds., *Elsevier Oceanogr. Ser.*, Vol. 46, 249-262.

Ruddick, B. R., and J.S. Turner, 1978. The vertical length scale of double-diffusive intrusions. *Deep-Sea Res.*, 26A, 903-913.

Stommel, H. and K.N. Fedorov, 1967. Small-scale structure in temperature and salinity near Timor and Mindanao. *Tellus*, 19, 306-325.

Thorpe, S.A., P.K. Hutt and R. Soulsby, 1969. The effects of horizontal gradients on thermohaline convection. *J. Fluid Mech.*, 38, 375-400.

Toole, J. M. and D.T. Georgi, 1981. On the dynamics and effects of double-diffusively driven intrusions. *Prog. Oceanogr.*, 10, 121-145.

Turner, J.S. 1978. Double diffusive intrusions into a density gradient. *J. Geophys. Res.*, 83, 2887-2901.

Walsh, D., and B. R. Ruddick, 1995. Double-diffusive interleaving: the influence of non-constant diffusivities. J. Phys. Oceanogr. 25(3), 348-358.

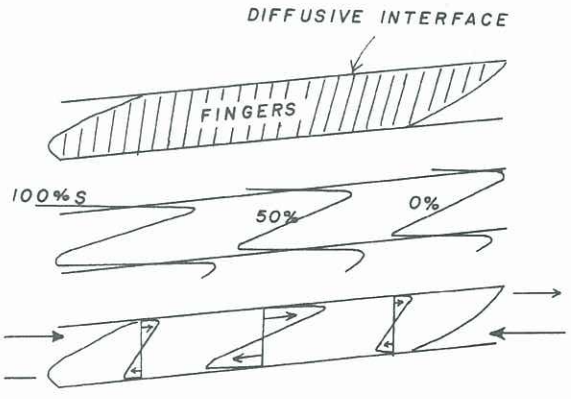

Figure 1: Cartoon of laboratory thermohaline intrusions showing, from top to bottom: the alternating diffusive interfaces and finger regions, sloping upward from the high-S side of the front; the contours of S concentration relative to the cross-frontal S-contrast; the velocity structure within the interleaving layers.

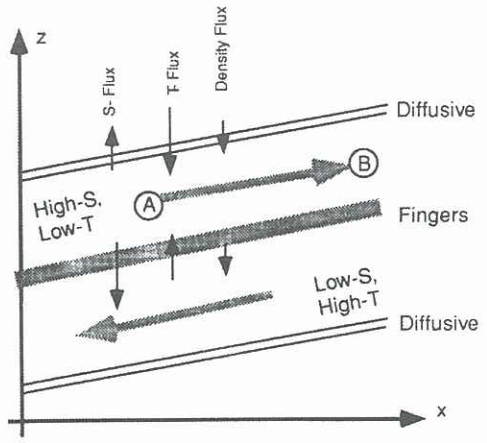

Figure 2: Illustration of the role of vertical double-diffusive fluxes in thermohaline intrusions. Both the finger and double-diffusive fluxes cause the high-S layer to lose S and T, but the layer will become lighter or denser according to whether the finger or diffusive buoyancy flux is larger.

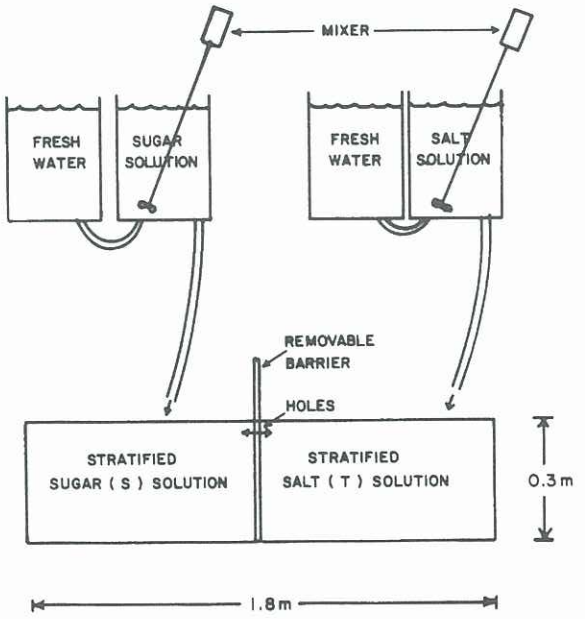

Figure 3: Schematic of the experimental tank and the two sets of filling apparatus used to create corresponding density stratifications on either side of the removable barrier.

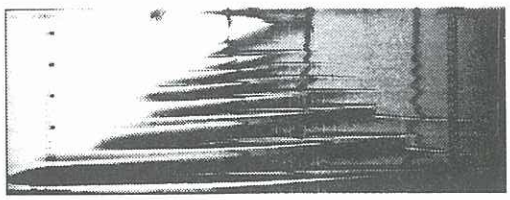

Figure 4: Shadowgraph of a typical experiment, showing the alternating diffusive interfaces and finger regions sloping up to the right. The vertical scale and speed of advance of the layers is larger near the bottom of the tank where the cross-frontal $T - S$ contrast is largest.

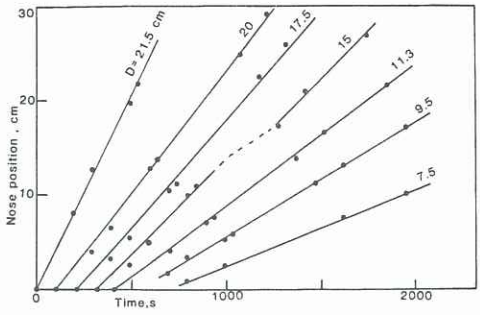

Figure 5: Position of the noses from one experiment plotted against time. Both axes have been offset arbitrarily. The depth D below the free surface, where the S–contrast is zero, is indicated on each curve. Note the merging of some layers (dashed line segment), causing temporary interruptions to nose progression.

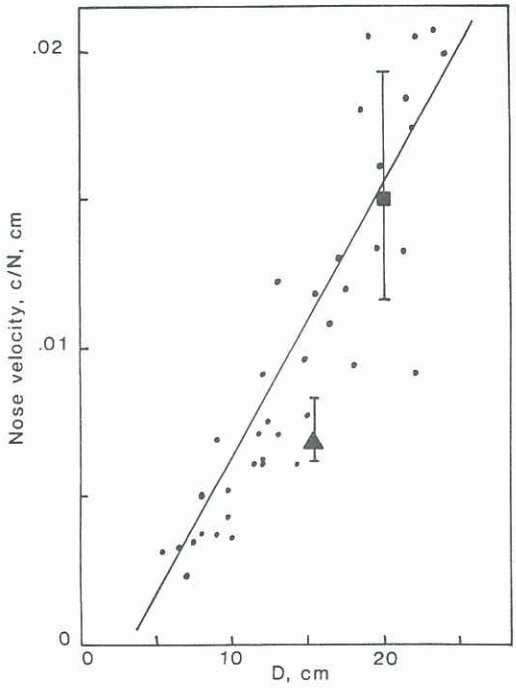

Figure 6: Intrusion nose velocity c, normalized by N, vs D from several experiments. The solid square and triangle indicate the average nose velocities from experiments in which $\beta\Delta S$ was constant with depth. The error bars indicate the deviation of nose speed within those experiments.